environments

MDPI

Technical Note

Seasonal Spectral Separation of Western Snowberry and Wolfwillow in Grasslands with Field Spectroradiometer and Simulated Multispectral Bands

Irini Soubry * and Xulin Guo

Department of Geography and Planning, University of Saskatchewan, 117 Science Place, Saskatoon, SK S7N 5C8, Canada; xug991@mail.usask.ca
* Correspondence: irini.soubry@usask.ca

Abstract: Woody plant encroachment (WPE), the expansion of native and non-native trees and shrubs into grasslands, has led to degradation worldwide. In the Canadian prairies, western snowberry and wolfwillow shrubs are common encroachers, whose cover is currently unknown. As the use of remote sensing in grassland monitoring increases, opportunities to detect and map these woody species are enhanced. Therefore, the purpose of this study is to identify the optimal season for detection of the two shrubs, to determine the sensitive wavelengths and bands that allow for their separation, and to investigate differences in separability potential between a hyperspectral and broadband multispectral approach. We do this by using spring, summer, and fall field-based spectra of both shrubs for the calculation of spectral separability metrics and for the simulation of broadband spectra. Our results show that the summer offers higher discrimination between the two species, especially when using the red and blue spectral regions and to a lesser extent the green region. The fall season fails to provide significant spectral separation along the wavelength spectrum. Moreover, there is no significant difference in the results from the hyperspectral or broadband approach. Nevertheless, cross-validation with satellite imagery is needed to confirm the current results.

Keywords: western snowberry; *Symphoricarpos occidentalis*; wolfwillow; *Elaeagnus commutata*; spectral separability; seasonal variation; grassland; woody plant encroachment

Citation: Soubry, I.; Guo, X. Seasonal Spectral Separation of Western Snowberry and Wolfwillow in Grasslands with Field Spectroradiometer and Simulated Multispectral Bands. *Environments* **2021**, *8*, 60. https://doi.org/10.3390/environments8070060

Academic Editors: Yu-Pin Lin, Teiji Watanabe, Ram Avtar and Li-Pei Peng

Received: 6 May 2021
Accepted: 18 June 2021
Published: 22 June 2021

1. Introduction

Grasslands are among the largest ecosystems in the world, providing important ecologic and economic services [1]; however, they face multiple threats from climate change and human activity (e.g., conversion to cropland, biodiversity loss, expansion of invasive species), which can lead to their degradation [2]. Woody plant encroachment (WPE) has become an important issue for grasslands in recent years. It is related to the expansion of native and non-native trees and shrubs into grasslands [3], and has been connected to changes in primary productivity, nutrient cycling, energy flow, the structure and function of the ecosystem [3]; these all lead to issues in rangeland management and livestock production. There exist various definitions of woody plant encroachment in the literature; except for the term "woody plant encroachment", the terms "woody plant invasion" [4], "woody thicketization" [5], "woody plant expansion" [6], "invasion of woody weed" [7], "xerification" [8], and "invasion of shrubs" [9] are also used. This is because WPE is a global phenomenon, and definitions depend on the precipitation gradient of the region. In particular, WPE occurs in the grasslands of the south-central and southwestern United States (mesquite and creosote brush) [10], North America (juniper) [11], South America (honey locust) [12], Southern Africa (*Acacia* and *Grewia* spp.) [13], Australia [14], Mongolia [15], Europe [16], and the Arctic (willow and *Alnus* spp.) [17].

WPE also takes place in the Canadian prairies, where tree encroachment (e.g., aspen, willow) has received more attention in the literature [18–23]. For instance, trembling

aspen (*Populus tremuloides*) is the dominant tree species encroaching on grasslands and pastures within the aspen parkland ecoregion in western Canada [24]. Other species, such as willow (*Salix* spp.) and Balsam poplar (*Populus balsamifera*) are also encroachers, but to a lesser extent. Thorny buffaloberry is an encroaching species in Alberta [25]. The most common encroachers that occur throughout several Canadian prairie ecoregions (i.e., aspen parkland, moist mixed grassland, mixed grassland) are western snowberry (*Symphoricarpos occidentalis*) [26] and wolfwillow (*Elaeagnus commutate*). Therefore, these two shrub species will be the main focus of this research, since they have been less studied. Moreover, the province of Saskatchewan will be our study area, since it includes the three previously mentioned ecoregions. An example of an encroaching shrub species in the rangelands of southern Saskatchewan is western snowberry, found in the commercial rangelands and provincial pastures of the Grand Coteau region and Weyburn. One can also find western snowberry and wolf willow in Burstall rangelands, the Northeast Swale of Saskatoon, Meewasin Valley, Kernen Prairie, and most of Saskatchewan's southern provincial parks (pers. comm. Mr. Merek Wigness, Dr. Eric Lamb, Dr. Thuan Chu, and pers. observ.). It is understood that shrub encroachment is either already an issue or might become an issue in most of southern Saskatchewan's rangelands. Nevertheless, the cover of these species within the prairies is currently unknown.

It is clear that maintaining grassland health is crucial, especially when food scarcity is estimated to rise, and sustainable management solutions are needed [27]. This fits within the United Nations Sustainable Development Goal 15.3 on "Land degradation neutrality". Remote sensing can be used with success to fulfill this aim by mapping the spatiotemporal distribution of various encroaching species with the use of different methods and datasets [28,29]: for instance, to detect two *Acacia* species from hyperspectral imagery with the use of differences in their phenology in Namibia [30], to classify *Prosopis* and *Vachellia* spp. with an object-based approach in Kenya [31], to detect redberry juniper and honey mesquite in north central Texas with spectral contrast of a three-band aerial image [32], to classify three woody invasive species with spectral, textural, and structural features in Chile [33], and to detect six types of woody species with multispectral aerial imagery and LiDAR derived heights in the Netherlands [34]. Overall, for species-specific detection, high spatial resolution is necessary. However, the use of high spectral and temporal resolution could compensate for the lack of spatial resolution, and is more preferable for regional and landscape scale mapping. Furthermore, when thinking about the phenological behavior of each woody species of interest, it might be necessary to define the optimal detection timeframe within the growing season for each one. We therefore focus our study on a seasonal spectral approach. Hyperspectral data have been used to detect WPE species due to their wide band range, which allow for the detection of finer spectral differences. In addition, field-based hyperspectral measurements offer the opportunity to fine-tune spaceborne and airborne sensors for larger-scale shrub species mapping by selecting appropriate spectral bands and regions with spectral separability metrics and statistics (e.g., InStability Index, Transformed Divergence, etc.). Afterwards, one can define remote sensing indices that use these bands and apply a broader land cover classification.

To our knowledge, no study has looked at seasonal hyperspectral and multispectral differences between western snowberry and wolfwillow for their potential detection with remotely sensed data, which can facilitate WPE management in the Canadian prairies. Therefore, the main purpose of this study is to derive the seasonal sensitive spectral regions for separation between western snowberry and wolfwillow shrubs in grasslands. Our main objectives are (1) to identify the optimal season for detection of the two shrub cover types, (2) to determine the sensitive wavelengths and bands that allow for their separation, and (3) to investigate differences in separability potential between a hyperspectral and broadband multispectral approach.

2. Materials and Methods

2.1. Study Area and Case Study Species

The study area is the University of Saskatchewan's Kernen Crop Research Farm (Saskatoon, Canada) in which WPE is an issue in its prairie stand. This area has a native remnant fescue prairie with common mixed prairie species which spans over 1.3 km^2 at about 8 km NE of Saskatoon in Saskatchewan (52°10″ N, 106°33″ W, 510 m mean elevation) [35,36] (Figure 1). More information about the study area can be found in [37]. This site was chosen as representative of a grassland ecosystem and could be easily accessed during the pandemic restriction. The shrubs that are present consist of western snowberry (*Symphoricarpos occidentalis* Hook.) [38], wolf-willow (*Elaeagnus commutata* Bernh. Ex Rydb.), and wild prairie rose (*Rosa arkansana*) [39,40]. In this study, we focus on western snowberry and wolf-willow, which are encroaching species in the site (Figure 2).

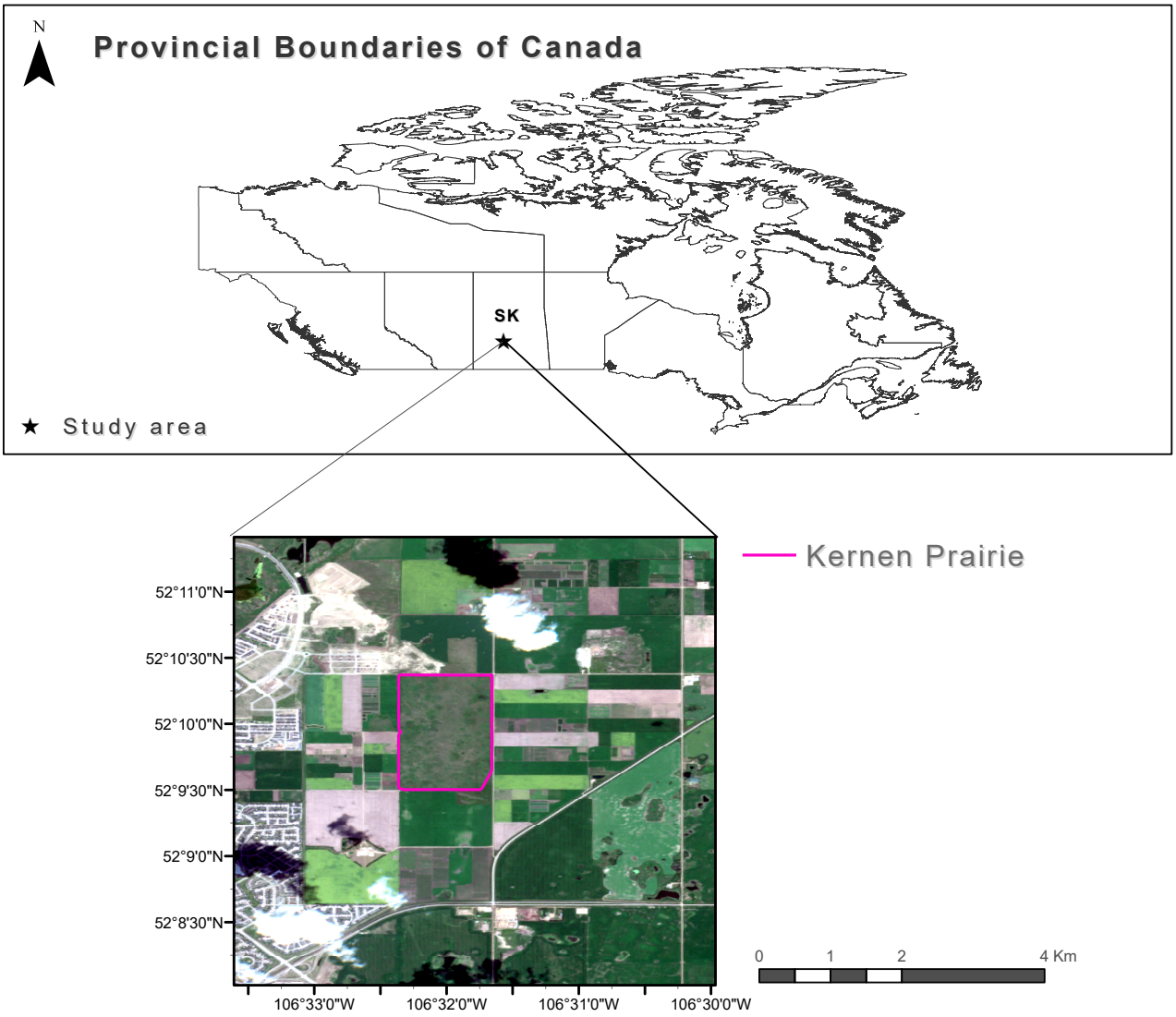

Figure 1. Location of Kernen Prairie within the provincial boundaries of Saskatchewan (SK), Canada (**upper figure**), and on a Sentinel-2 image of 11 July 2020 (**lower figure**). Source of Canadian Provincial Boundaries: Statistics Canada (Open-Government License—Canada) [41], source of Sentinel-2 image: ESA ('Copernicus Service information 2020' for Copernicus Service Information) [42], source of Kernen Prairie boundary layer: Department of Plant Science, University of Saskatchewan (Dr. Eric Lamb).

(**a**) (**b**)

Figure 2. Shrub species present in study area: (**a**) western snowberry (source: personal collection, Kernen Prairie, Saskatoon, Saskatchewan, CA, 11 June 2020), (**b**) wolfwillow (source: personal collection, Cypress Hills Interprovincial Park, Saskatchewan, CA, 18 August 2020).

Western snowberry (*Symphoricarpos occidentalis*) or otherwise western wolfberry, wolfberry, or buckbrush, occurs throughout most of the southwestern Canadian provinces and northern United States Great Plains [43]. It is a deciduous rhizomatous short shrub (0.3–1.5 m) that forms dense colonies between 1 and 200 m [44]. It is dominant in Saskatchewan along temporarily flooded shrublands of the northern Great Plains [45], next to water streams, at the base of steep slopes with runoff, and on north or east facing slopes [46]. This shrub is common in the mixed-grass prairies. Specifically in Saskatchewan, it was found that western snowberry had lower density in areas with less water availability in comparison to sites with higher water availability [47]. This species grows in continental climates with extreme temperatures and light to moderate rainfall [48], and it can survive moderate drought [49]. Western snowberry grows on most soil types (e.g., silt, clay, fine sand, rocky substrates, and rich loams) apart from loose sands [50]. Further, it is common on mild alkaline to slightly acidic soils [51]. Western snowberry does well after disturbance, such as fire [38], and grazing [50]. When it encroaches into grasslands, it leads to a decline in forage [52], as it shades out grasses [40], and facilitates the establishment of trees, such as trembling aspen [53]. For the Northern Great Plains, fire cessation has led to the encroachment of western snowberry into the mixed-grass prairie [53]. Generally, western snowberry can be an increaser in many productive range sites, or a decreaser on other ecosites [54].

Wolfwillow (*Elaeagnus commutata*) or silverberry belongs to the Elaeagnaceae family and, native to south Canada, it is a deciduous rhizomatous perennial shrub (1–4 m tall) [55]. It forms thickets or loose colonies, and one of the ecosystems in which it occurs is the plains grasslands [56]. This species can be found along streams, and near springs, while it can grow on different slopes, elevations, aspects, and soil conditions [49]. It thrives in loamy soils, but is also found in dry, sandy, and gravel soils [57]. Specifically, in the mixed-grass prairie, it is frequently found together with western wheatgrass, needlegrass, and rough fescue [58]. In Saskatchewan, it is common on native fescue grasslands [59]. In particular, wolfwillow had minor cover in the 1950s, in contrast to its currently wide distribution [60]. Wolfwillow adapts well to areas that are disturbed. This is why it is increasing on rangelands that are overgrazed by cattle [58]. Wolfwillow has the ability to spread fast through rhizomes [60], but it seems to not recover fast after burning [59]. It is shade intolerant [61], justifying its common presence in open vegetation. This species is also resistant to drought, wind, and extreme cold temperatures up to −40 °C [57]. Wolfwillow

might also increase the available forage for cattle by fixing nitrogen, making it available to other surrounding species and plants [49]. Hence, the complete eradication of wolfwillow should be avoided [62]. Nevertheless, it seems that areas with wolfwillow are grazed less than half as much as neighboring grass areas that do not have this species [62].

2.2. Data Collection

We collected field hyperspectral data three times in the 2020 growing season (spring, summer, and fall). This was done with the use of a spectroradiometer (ASD field-portable FieldSpec Pro, Malvern Panalytical Inc., Boulder, CO, USA) between 10:00 and 14:00 during clear sky sunny weather conditions to maintain a stable ratio between diffuse and incoming solar radiation. The spectroradiometer collects between 350 and 2500 nm with a 1 nm band range. Reference measurements with a Spectralon panel were taken at least every 15 min. Measurements included the collection of shrub endmembers (i.e., wolfwillow and snowberry) that are encroaching in the study area. The spectroradiometer was placed close to the shrubs and at least 10 samples for each shrub species were measured to ensure the plant's spectral variation was captured (i.e., leaves, branches). This allows us to have a spectral signature for ~100% shrub cover of the existing species in the study area.

2.3. Data Processing

2.3.1. Calculation of Separability Metrics

For all collected spectral data, we removed the water absorption regions between 1350–1430 nm, 1750–1980 nm, and 2330–2500 nm, which caused noise in the data. Next, we calculated the spectral separability between wolfwillow and western snowberry for each season and wavelength. Various separability metrics calculate how separable two groups are. We used five univariate statistic methods that are provided in the "separability" function of the "spatialEco" package in R [63]: namely, the M-Statistic (M) [64], Bhattacharyya distance (B) [65], Jeffries-Matusita (JM) distance [66], Divergence (D) [67], and Transformed Divergence (TD) [68]. These provide discrimination ability of each wavelength without taking into consideration their potential correlation [69].

Before the calculation of these separability metrics, a normality check to the wavelengths of each shrub per season was performed. For that purpose, we used the statistical Shapiro–Wilk test [70], which is considered more powerful than other statistical tests of normality [71], and has been used in similar studies [72]. Nevertheless, we also used visual methods (i.e., quantile–quantile plot, density plot), since the test's power might be lower with a small sample size (e.g., below 30). For all seasons, western snowberry was normal for 87–95% of the whole wavelength spectrum (non-normality along the red-edge region and far-SWIR (Shortwave Infrared) in all seasons, and blue region during fall), and for wolfwillow, between 97–100% (non-normality for blue region in spring, and far-SWIR in fall). Even though some wavelengths were partially not normal, we did not consider this as an issue for the current spectral separability analysis, since these wavelengths will be aggregated during broadband simulation and some might not contribute to the spectral separability of the two shrubs. Furthermore, following a non-parametric separability approach for this small number of samples could result in larger biases than the slight deviation from normality for at most 13% of the current dataset.

2.3.2. Thresholding and Selection of Important Wavelength Regions

To select the final wavelength regions capable of separating western snowberry and wolfwillow, we had to identify cut-off thresholds for each of the separability metrics calculated. TD can have values between 0 and 2, with 2 providing maximum separability potential between groups. TD scales the divergence statistic, which looks at the difference between two distributions from their mean values of the log-likelihood ratio [73]. Previous research shows that TD provides good separability when it has values above 1.8 [74] or 1.9 [75]. Similarly, when TD has values between 1.5 and 1.8 or 1.9, two groups have moderate separation, whereas those with values below 1.5 have poor separation [74,75].

We therefore consider this classification from the literature for our own study (Table 1). JM is the scaled version of the B distance, which measures the divergence between two groups through the calculation of their cosine angle [65]. Since JM also follows a scale from 0 to 2, we used the same threshold rules for this metric. Furthermore, when the M-statistic is >1, it is considered that there is good separation [64], so we used this approach, although for this statistic it is hard to define an intermediate separation level, because there is no upper limit. Similarly, one cannot define thresholds for the B and D statistics, since they continue to increase without an upper bound. Therefore, these statistics (B, D) only give a general idea of the important contributing wavelength regions towards the separability of the two shrubs. The final wavelength regions for which both the TD and JM have values above or equal to 1.8 were considered as having good separation. A similar ensemble approach was used for the moderate separability regions.

Table 1. Separability threshold values (based on Kaufman and Remer [64], Campbell [74], and Bindel et al. [75]).

Separability Statistic	Threshold Value	Separability Class
M-Statistic	>1	Good
	≤1	Poor
Transformed Divergence & Jeffries–Matusita Distance	≥1.8	Good
	1.51–1.79	Moderate
	≤1.5	Poor

2.3.3. Broadband Spectral Difference between Shrub Species

We resampled the seasonal shrub spectra into the broadband Landsat 8, Sentinel-2A, and Sentinel-2B bands with the use of their spectral response functions. In particular, we performed the broadband simulation within the "hsdar" package in R with the use of the "spectralResampling" function [76]. To determine if there was a significant difference between the two shrub groups in each season per simulated broadband, we performed multiple two-sampled *t*-tests assuming unequal variance per band. We used this test since the variances were unequal for some bands (based on results from a two-sided F-test) and due to the unequal sample size between the two shrub groups. We report the results of the *t*-tests in a table with two levels of adjusted *p*-value significance: below 0.05, and below 0.01. We further performed the same analysis as in Sections 2.3.1 and 2.3.2 with the broadband spectra. Before running these processes, we performed the Shapiro–Wilk test [70] to check if the assumptions of normality held. The results of the test showed that all simulated broadband for both shrubs had a normal distribution.

3. Results

3.1. Seasonal Spectra of Shrub Species

One can see the average seasonal spectral reflectance for each shrub species in Figure 3a–c. The spectral signatures for both species are openly available through Figshare (https://doi.org/10.6084/m9.figshare.14541597.v1 (accessed on 21 June 2021)). The reflectance of wolfwillow in the visible region (350–700 nm) is higher than that of western snowberry for all seasons, and so is the reflectance in the shortwave infrared (SWIR) region (1450–2350 nm). Rather noticeable is the lack of absorption for wolfwillow in the blue region (350–500 nm), which could be explained by the grey-blue appearance of its leaves (Figure 1). Further, the SWIR reflectance for western snowberry decreases slightly from spring to summer, and increases again during fall, whereas it increases throughout the seasons for wolfwillow. These patterns could be related to the seasonal leaf water content of each shrub. For the near infrared (NIR) region, western snowberry has higher reflectance than wolfwillow during spring, after which wolfwillow takes over for the summer and fall. Based on their different spectral signatures, it should be possible to detect each shrub.

The separability metrics can indicate how well each of the wavelengths contribute to this separation.

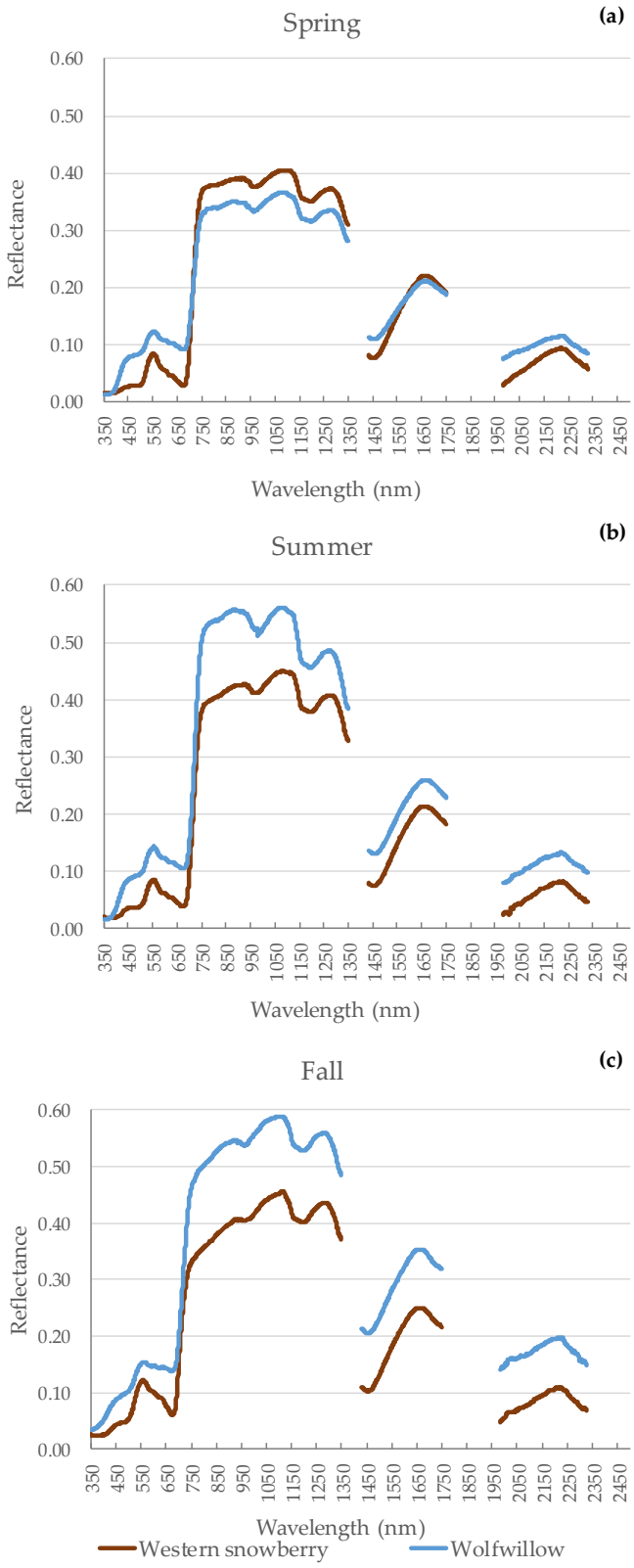

Figure 3. Average spectral signatures for western snowberry and wolfwillow in (**a**) spring, (**b**) summer, and (**c**) fall (water absorption regions between 1350–1430 nm, 1750–1980 nm, and 2330–2500 nm have been removed; the data are available on Figshare https://doi.org/10.6084/m9.figshare.14541597.v1 (accessed on 21 June 2021).

3.2. Hyperspectral Separability of Shrub Species

Seasonal separability between western snowberry and wolfwillow: When looking at the separability metrics for the two shrub species (Figure 4), we can see that separability is higher for the visible wavelengths during spring and summer, while it is higher for the far-SWIR region during fall. When looking at the whole wavelength spectrum, we see that the highest separability values correspond to the summer season, while the lowest to the fall season. In addition, TD and JM have similar results, with JM having lower values for most wavelength regions during spring and fall. Moreover, the M and B metrics show similar responses to the previous two; however, on a different scale, while the D metrics show some dissimilarity in the visible wavelength responses for spring and summer. The pattern similarity between all metrics provides additional reassurance towards trusting the thresholded results of the TD, JM, and M metrics.

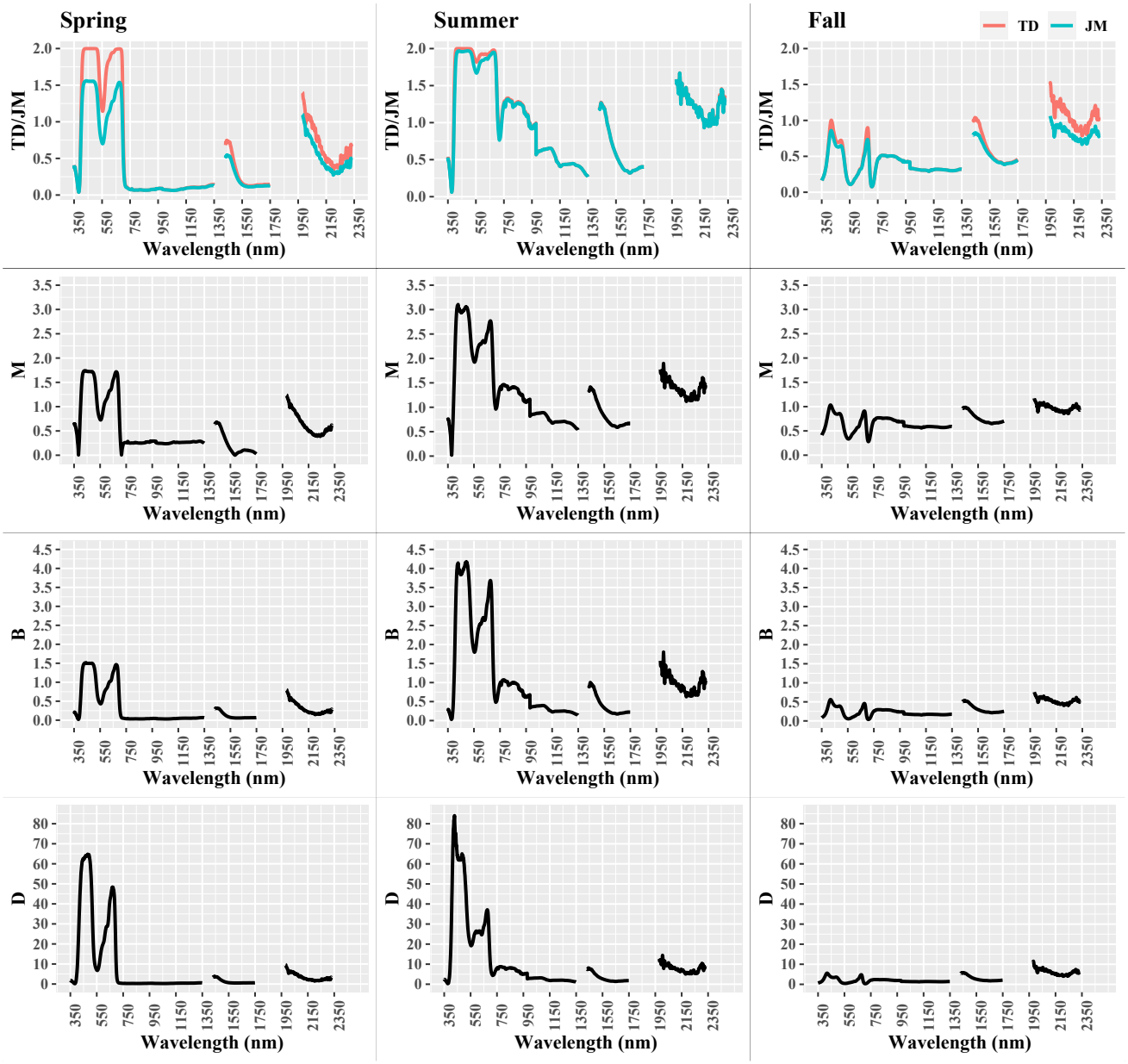

Figure 4. Seasonal spectral separability metric results between western snowberry and wolfwillow across all hyperspectral wavelengths (Transformed Divergence (TD), Jeffries–Matusita (JM) distance, M-Statistic (M), Bhattacharyya distance (B), Divergence (D); water absorption regions between 1350–1430 nm, 1750–1980 nm, and 2330–2500 nm have been removed).

Based on the set thresholds (Table 1), the highest number of wavelengths that offer good separation are found in the summer (i.e., 17.57% for TD, 14.45% for JM), whereas only 0.12% of wavelengths offer moderate separation with the TD metric during fall (Table S1, Supplementary Materials). This is an initial indication towards the preferable selection of the summer season for the detection of both shrubs. Overall, the TD metric suggests a higher number of wavelengths that offer good separability for the two shrubs compared to the JM metric (13.25% vs. 0.00% in the spring, and 17.57% vs. 14.45% in the summer), whereas the M metric cannot distinguish moderate or good separation.

Wavelength regions sensitive to shrub species separation: To identify the wavelength regions that are important for the detection of each shrub species, we applied an ensemble method, in which the TD- and JM-defined wavelengths that are classified as moderate or good under both metrics are selected (Table 2). The reason for this is that both metrics allow for better interpretation and separation based on threshold establishment due to their upper limit (i.e., 2). The selected wavelength bands belong to certain spectral regions, and those that were below 10 nm wide were removed (e.g., some regions in the SWIR in the summer). The ensemble method could not be applied for the fall season, as none of the metrics included any wavelengths in the moderate or good category.

Table 2. Seasonal wavelength bands and spectral regions that offer moderate and good separation between western snowberry and wolfwillow based on thresholds established in Table 1 (B = Blue, R = Red, RE = Red-Edge, SWIR = Shortwave infrared).

Separability between Western Snowberry and Wolfwillow				
Season	**Wavelength Areas**			
	Moderate		**Good**	
	(nm)	**Category**	**(nm)**	**Category**
Spring	/	/	409–525	B
	/	/	590–693	R/RE
Summer	532–577	G	406–531	B
	1981–1991	SWIR	578–692	R/RE
Fall	/	/	/	/

In detail, the spring spectral regions in the blue (409–525 nm) and red-red edge (590–693 nm) offer good separation between the two species. For the summer season, the blue and red-red edge regions continue to offer good separation. In addition, the green region (532–577) is able to moderately separate the two species, since the reflectance of wolfwillow around the green peak is about 0.05 units higher than it was in spring. Furthermore, a narrow wavelength region in the far-SWIR (1981–1991 nm) offers moderate separation. During fall, both species are at the start of senescence, and although we do see some differences in their spectral signature and a few peaks in the separability metrics, these values are not high enough to allow for moderate or good separation.

3.3. Broadband Simulation and Shrub Species Spectral Band Difference

Broadband simulation: The mean values for each Landsat 8 and Sentinel-2A band per shrub species and season are presented in Table S2 (Supplementary Materials). The results for Sentinel-2B are very similar and are available in Table S3 (Supplementary Materials).

Shrub species spectral differences (two-sample t-tests): The two-sampled *t*-test *p*-values for each Landsat 8 and Sentinel-2A band per shrub species and season are presented in Table 3. Since the Sentinel-2B reflectance values are almost the same as those of Sentinel-2A, we did not perform *t*-tests on these. Several conclusions can be drawn from these results. First, we can see that the SWIR 1 region is not significantly different between the two species during spring. The same holds for the red edge (RE) 3 and RE 4 band of Sentinel-2A during spring, and the RE 1 band during fall. Season wise, we can see that all bands are significantly different during the summer season, whereas the blue, red and SWIR 1 bands

are important for both sensors during all three seasons. Although the different *p*-values give an indication of the strength of these differences, the separability metrics offer higher precision towards the level of separation that each band can offer.

Table 3. Two-sampled *t*-test *p*-values per Landsat 8 and Sentinel-2A band for each shrub species and season (B-Blue, G-Green, R-Red, RE-Red Edge, W. Vap.-Water Vapour, SWIR = Shortwave infrared). Red colored values are significant *p*-values within the 99% confidence interval (CI) (*p*-value < 0.01) and yellow values are those that are significant within the 95% CI, but not in the 99% CI (*p*-value between 0.01 and 0.05).

Two-Sample *t*-Test *p*-Values															Yel.	<0.05	Red	<0.01
Season	**Landsat-8**						**Sentinel-2A**											
	B	**G**	**R**	**NIR**	**SWIR 1**	**SWIR 2**	**B**	**G**	**R**	**RE 1**	**RE 2**	**RE 3**	**NIR**	**RE 4**	**W. Vap.**	**SWIR 1**	**SWIR 2**
Spring	0.000	0.000	0.000	0.049	0.748	0.001	0.000	0.000	0.000	0.006	0.046	0.051	0.049	0.052	0.027	0.702	0.001
Summer	0.000	0.000	0.000	0.000	0.005	0.000	0.000	0.000	0.000	0.000	0.000	0.000	0.000	0.000	0.000	0.006	0.000
Fall	0.000	0.035	0.000	0.000	0.001	0.000	0.000	0.047	0.000	0.077	0.001	0.000	0.000	0.000	0.000	0.001	0.000

Shrub species broadband spectral separability: The spectral separability metrics calculated for the Landsat 8 broadband simulation are depicted in Figure 5 for each band and season, and in Figure 6 for Sentinel-2A. It is clear that the bands in the visible spectrum are more important during spring and summer, whereas the SWIR-2 band seems to have the highest separability during fall. However, these values are much lower during fall compared to the other two seasons, for which summer shows the highest values for most metrics and bands. These results go in line with the outcomes of Section 3.2 and Figure 4. Based on the thresholds from Table 1 and the ensemble approach, we can see that Landsat 8 offers moderate separability between the two shrubs with the blue and red band. However, for Sentinel-2, only TD shows good separability for those two bands, and not JM (Table 4). In the summer, the blue and red bands of both sensors offer good separation, and the green band moderate, whereas none of the bands offer any level of separation in the fall. These findings agree with the previous ones from Section 3.2 regarding the selection of the summer season for the detection of wolfwillow and western snowberry, and the fact that the TD metric suggests higher separability than JM during spring.

Table 4. Seasonal wavelength bands that offer moderate and good separation between western snowberry and wolfwillow with Landsat 8 and Sentinel-2A simulated data (B = Blue, R = Red, G = Green).

Separability between Western Snowberry and Wolfwillow				
Season	**Wavelength Bands**			
	Moderate		**Good**	
	Landsat 8	**Sentinel-2A**	**Landsat 8**	**Sentinel-2A**
Spring	B R	/	/	/
Summer	G	G	B R	B R
Fall	/	/	/	/

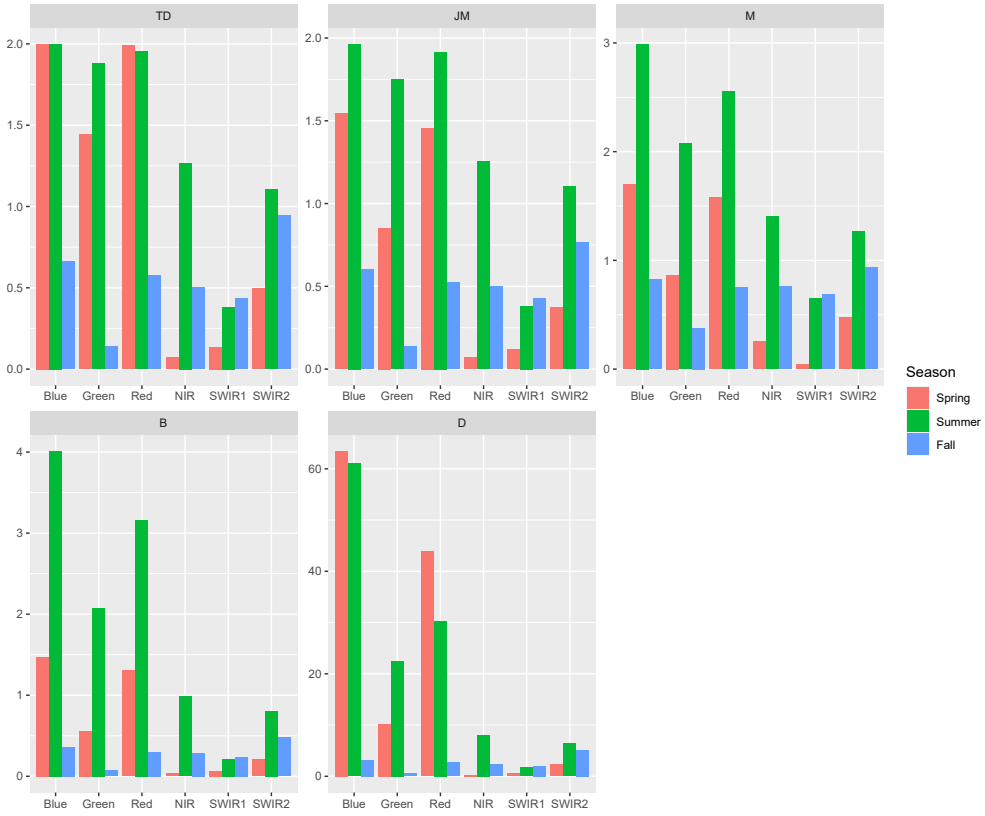

Figure 5. Seasonal spectral separability metric results between western snowberry and wolfwillow across selected Landsat 8 bands (Transformed Divergence (TD), Jeffries–Matusita (JM) distance, M-Statistic (M), Bhattacharyya distance (B), Divergence (D)).

Figure 6. Seasonal spectral separability metric results between western snowberry and wolfwillow across selected Sentinel-2A bands (Transformed Divergence (TD), Jeffries–Matusita (JM) distance, M-Statistic (M), Bhattacharyya distance (B), Divergence (D)).

4. Discussion and Conclusions

Our results from the hyperspectral metrics, broadband metrics and two-sampled *t*-tests show that the summer season is the optimal one for the spectral separation of western snowberry and wolfwillow, as it has the highest number of significantly different spectral regions and bands. This is reasonable, since the summer is the peak of the growing season with the highest photosynthetic activity, during which differences between shrub species could become more obvious. For this reason, the summer season has been frequently selected for data acquisition when separating shrub species due to the higher vigor of vegetation in that season [31,33,34,77]. Summer months have also shown better discrimination abilities compared to other months—even for separating an evergreen and a deciduous species [29]. As for the optimal wavelength regions and bands, both blue and red are important, and more so in the summer. These two regions are influenced by stronger chlorophyll absorption for western snowberry compared to wolfwillow, based on their spectral signature. On the other hand, the green peak (around 550 nm) is similar for both shrubs, and is therefore not useful for classification in the spring. Nevertheless, this spectral region is moderately important during summer, where the reflectance of wolfwillow is significantly higher than that of western snowberry. Lastly, in the far-SWIR, there is moderate separation for a narrow hyperspectral region in spring, which is not represented in the broadband simulations. Although this region is significantly different in all seasons based on the two-sampled *t*-test, it is not strong enough to reflect its difference in the separability metrics. This region is most possibly related to the differences in water and moisture absorption between the two species.

Overall, when looking at the differences between the hyperspectral and broadband results for the separation of the two shrubs, we notice that the results are almost the same, except for a narrow region in the far-SWIR, which is not included in the broadband results. This leads us to the conclusion that hyperspectral data would not really improve the classification results for our specific study purposes, and that use of Landsat 8 or Sentinel-2 data would suffice. In addition, the increased number of spectral bands that Sentinel-2 data provide do not offer enhanced detection capabilities, since the NIR region that includes the red-edge bands is not one of the sensitive regions for western snowberry and wolfwillow classification throughout the seasons.

However, we must point out that our current simulated broadband results represent the leaf/branch scale and not the canopy scale. The reflectance properties of the two shrubs could be different at that scale due to canopy architecture, such as leaf angle distribution, density, biomass, and leaf area index, in which shadows and occlusions also play a role. In addition, these simulations do not represent satellite data conditions, which are strongly affected by the atmosphere, and which capture the land surface at a broader scale, in which topography also has a significant role. Furthermore, since Landsat and Sentinel-2 data capture the surface at a broader scale (10–30 m), each image pixel is usually a mixture of different land cover types (e.g., woody plants, grass, bare ground, rock). This is especially the case when WPE is at an early stage. Overall, grasslands can undergo different WPE stages (i.e., early, moderate, or advanced), resulting in different woody cover within an image pixel [78]. A field-based study showed that the earliest WPE that could be identified was when it reached between 10% and 25% of an image pixel [37]. However, more research with remotely sensed imagery is needed to verify this result. Nevertheless, even with mixed pixels, there exists a number of spectral unmixing techniques that could enhance WPE species specific mapping with coarse resolution pixels [79]. With this technique, each pixel gets assigned to a fraction of its land covers, which are defined by endmembers. Two endmember classes that could be used for that purpose are the spectral signatures of western snowberry and wolfwillow that were used in this study. For the above reasons, the optimal season and bands detected in the current study for separation between the two woody shrubs might not coincide with their actual detection on the landscape. Therefore, the current results should be cross-validated with satellite-based remote sensing data, such as Landsat 8 and Sentinel-2. We plan to implement this in future research that will establish

specific broadband multispectral indices optimally correlated with the two shrub species of this study, and with research that will investigate potential improvements in their detection with spectral unmixing techniques.

Supplementary Materials: The following are available online at https://www.mdpi.com/article/10.3390/environments8070060/s1, Table S1: Wavelength classification according to separability thresholds for the seasonal Transformed Divergence (TD), Jeffries–Matusita (JM), and M-statistic (M) metrics, Table S2: Mean simulated reflectance value (%) per Landsat 8 and Sentinel-2A band for each shrub species and season (B-Blue, G-Green, R-Red, RE-Red Edge, W. Vap.-Water Vapour, SWIR = Shortwave infrared), Table S3: Mean simulated reflectance value per Sentinel-2B band for each shrub species and season (B-Blue, G-Green, R-Red, RE-Red Edge, W. Vap.-Water Vapour, SWIR = Shortwave infrared).

Author Contributions: Conceptualization, I.S. and X.G.; methodology, I.S.; writing—original draft preparation, I.S.; writing—review and editing, X.G.; visualization, I.S.; supervision, X.G. All authors have read and agreed to the published version of the manuscript.

Funding: This research was funded by The Natural Sciences and Engineering Research Council of Canada (NSERC), grant number RGPIN-201603960.

Data Availability Statement: The data presented in this study are contained within the article and the supplementary material; and the collected field spectral data are openly available on FigShare at https://doi.org/10.6084/m9.figshare.14541597.v1 (accessed on 21 June 2021).

Acknowledgments: The authors would like to thank Eric Lamb for providing us with a suitable study area to conduct this research during COVID-19. We are especially thankful to Yunpei Lu for his assistance during fieldwork. We would also like to acknowledge the graduate student research team under Xulin Guo for their recommendations and suggestions during the research project and manuscript preparation. We further acknowledge funding from NSERC and the University of Saskatchewan. Lastly, we would like to thank our two anonymous reviewers for their fruitful suggestions during the revision process.

Conflicts of Interest: The authors declare no conflict of interest. The funders had no role in the design of the study; in the collection, analyses, or interpretation of data; in the writing of the manuscript, or in the decision to publish the results.

Abbreviations

B	Bhattacharyya distance
D	Divergence
JM	Jeffries–Matusita distance
M	M-Statistic
NIR	Near Infrared
RE	Red Edge
SWIR	Shortwave Infrared
TD	Transformed Divergence
WPE	Woody Plant Encroachment

References

1. Bengtsson, J.; Bullock, J.M.; Egoh, B.; Everson, C.; Everson, T.; O'Connor, T.; O'Farrell, P.J.; Smith, H.G.; Lindborg, R. Grasslands—More important for ecosystem services than you might think. *Ecosphere* **2019**, *10*, e02582. [CrossRef]
2. Gang, C.; Zhou, W.; Chen, Y.; Wang, Z.; Sun, Z.; Li, J.; Qi, J.; Odeh, I. Quantitative assessment of the contributions of climate change and human activities on global grassland degradation. *Environ. Earth Sci.* **2014**, *72*, 4273–4282. [CrossRef]
3. Archer, S.R.; Andersen, E.M.; Predick, K.I.; Schwinning, S.; Steidl, R.J.; Woods, S.R. Woody Plant Encroachment-Causes and Concequences. In *Rangeland Systems-Processes, Management and Challenges*; Briske, D.D., Ed.; Springer Series on Environmental Management; Springer: Cham, Switzerland, 2017; pp. 25–84.
4. Bond, W.J.; Midgley, G.F. A proposed CO_2-controlled mechanism of woody plant invasion in grasslands and savannas. *Glob. Chang. Biol.* **2000**, *6*, 865–869. [CrossRef]
5. Leite, P.A.; Wilcox, B.P.; McInnes, K.J. Woody plant encroachment enhances soil infiltrability of a Semiarid Savanna. *Environ. Res. Commun.* **2020**, *2*, 115005. [CrossRef]

6. Bond, W.J.; Midgley, G.F. Carbon dioxide and the uneasy interactions of trees and savannah grasses. *Philos. Trans. R. Soc. B Biol. Sci.* **2012**, *367*, 601–612. [CrossRef] [PubMed]
7. Price, J.N.; Morgan, J.W. Woody plant encroachment reduces species richness of herb-rich woodlands in southern Australia. *Austral Ecol.* **2008**, *33*, 278–289. [CrossRef]
8. Archer, S.; Boutton, T.W.; Hibbard, K.A. Trees in Grasslands: Biogeochemical Consequences Woody Plant Expansion. In *Global Biogeochemical Cycles in the Climate System*; Academic Press: Cambridge, MA, USA, 2001; pp. 115–137.
9. Liao, J.D.; Boutton, T.W.; Jastrow, J.D. Organic matter turnover in soil physical fractions following woody plant invasion of grassland: Evidence from natural 13C and 15N. *Soil Biol. Biochem.* **2006**, *38*, 3197–3210. [CrossRef]
10. Van Auken, O.W. Shrub Invasions of North American Semiarid Grasslands. *Annu. Rev. Ecol. Syst.* **2000**, *31*, 197–215. [CrossRef]
11. Leis, S.A.; Blocksome, C.E.; Twidwell, D.; Fuhlendorf, S.D.; Briggs, J.M.; Sanders, L.D. Juniper Invasions in Grasslands: Research Needs and Intervention Strategies. *Rangelands* **2017**, *39*, 64–72. [CrossRef]
12. Chaneton, E.J.; Mazia, N.; Batista, W.B.; Rolhauser, A.G.; Ghersa, C.M. Woody Plant Invasions in Pampa Grasslands: A Biogeographical and Community Assembly Perspective. In *Ecotones Between Forest and Grassland*; Springer: New York, NY, USA, 2012; pp. 115–144. ISBN 9781461437970.
13. Sankaran, M.; Hanan, N.P.; Scholes, R.J.; Ratnam, J.; Augustine, D.J.; Cade, B.S.; Gignoux, J.; Higgins, S.I.; Le Roux, X.; Ludwig, F.; et al. Determinants of woody cover in African savannas. *Nature* **2005**, *438*, 846–849. [CrossRef] [PubMed]
14. Eldridge, D.J.; Soliveres, S.; Bowker, M.A.; Val, J. Grazing dampens the positive effects of shrub encroachment on ecosystem functions in a semi-arid woodland. *J. Appl. Ecol.* **2013**, *50*, 1028–1038. [CrossRef]
15. Zhou, D.; Xia, Z.; Dong, L.; Wenjiang, H.; Dailiang, P.; Linsheng, H. Remote sensing identification of shrub encroachment in grassland in Inner Mongolia. *Transations Chin. Soc. Agric. Eng.* **2014**, *30*, 152–158.
16. Sanjuán, Y.; Arnáez, J.; Beguería, S.; Lana-Renault, N.; Lasanta, T.; Gómez-Villar, A.; Álvarez-Martínez, J.; Coba-Pérez, P.; García-Ruiz, J.M. Woody plant encroachment following grazing abandonment in the subalpine belt: A case study in northern Spain. *Reg. Environ. Chang.* **2018**, *18*, 1103–1115. [CrossRef]
17. Myers-Smith, I.H.; Hik, D.S.; Kennedy, C.; Cooley, D.; Johnstone, J.F.; Kenney, A.J.; Krebs, C.J. Expansion of canopy-forming willows over the twentieth century on Herschel Island, Yukon Territory, Canada. *Ambio* **2011**, *40*, 610–623. [CrossRef]
18. Bailey, A.A.W.; Irving, B.D.; Fitzgerald, R.D.; Journal, S.; May, N. Regeneration of Woody Species following Burning and Grazing in Aspen Parkland. *J. Range Manag.* **1990**, *43*, 212–215. [CrossRef]
19. Hilton, J.E.; Bailey, A.W. Cattle Use of a Sprayed Aspen Parkland Range. *J. Range Manag.* **1972**, *25*, 257–260. [CrossRef]
20. Peltzer, D.A.; Wilson, S.D. Hailstorm damage promotes aspen invasion into grassland. *Can. J. Bot.* **2006**, *84*, 1142–1147. [CrossRef]
21. Guedo, D.D.; Lamb, E.G. Prescribed burning has limited long-term effectiveness in controlling trembling aspen (populus tremuloides) encroachment into fescue grassland in prince albert national park. *Can. Field-Nat.* **2013**, *127*, 50–56. [CrossRef]
22. Fitzgerald, A.R.D.; Bailey, A.W. Control of Aspen Regrowth by Grazing with Cattle. *J. Range Manag.* **1984**, *37*, 156–158. [CrossRef]
23. Campbell, C.; Campbell, I.D.; Blyth, C.B.; Mcandrews, J.H. Bison Extirpatio May Have Caused Aspen Expansion in Western Canada. *Ecography* **1994**, *17*, 360–362. [CrossRef]
24. Moss, R.; Gardiner, B.; Bailey, A.; Oliver, G. *A Guide to Integrated Brush Management on the Western Canadian Plains*; Canada Manitoba Forage Council: Brandon, MB, Canada, 2008.
25. Dahl, R. Characterizing Thorny Buffaloberry (Shepherdia argentea) Encroachment into the Mixedgrass Prairie in Alberta, Western Canada. Available online: https://rri.ualberta.ca/2018/09/26/characterizing-thorny-buffaloberry-shepherdia-argentea-encroachment-into-the-mixedgrass-prairie-in-alberta-western-canada-regina-dahl-m-sc-2014/ (accessed on 11 December 2020).
26. Bai, Y.; Colberg, T.; Romo, J.T.; McConkey, B.; Pennock, D.; Farrell, R. Does expansion of western snowberry enhance ecosystem carbon sequestration and storage in Canadian Prairies? *Agric. Ecosyst. Environ.* **2009**, *134*, 269–276. [CrossRef]
27. Schellberg, J.; Verbruggen, E. Frontiers and perspectives on research strategies in grassland technology. *Crop Pasture Sci.* **2014**, *65*, 508–523. [CrossRef]
28. Becker, R.H.; Zmijewski, K.A.; Crail, T. Seeing the forest for the invasives: Mapping buckthorn in the Oak Openings. *Biol. Invasions* **2013**, *15*, 315–326. [CrossRef]
29. Somers, B.; Asner, G.P. Invasive species mapping in hawaiian rainforests using multi-temporal hyperion spaceborne imaging spectroscopy. *IEEE J. Sel. Top. Appl. Earth Obs. Remote Sens.* **2013**, *6*, 351–359. [CrossRef]
30. Oldeland, J.; Dorigo, W.; Wesuls, D.; Jürgens, N. Mapping bush encroaching species by seasonal differences in hyperspectral imagery. *Remote Sens.* **2010**, *2*, 1416–1438. [CrossRef]
31. Ng, W.T.; Rima, P.; Einzmann, K.; Immitzer, M.; Atzberger, C.; Eckert, S. Assessing the potential of sentinel-2 and pléiades data for the detection of *Prosopis* and *Vachellia* spp. in Kenya. *Remote Sens.* **2017**, *9*, 74. [CrossRef]
32. Mirik, M.; Chaudhuri, S.; Surber, B.; Ale, S.; James Ansley, R. Detection of two intermixed invasive woody species using color infrared aerial imagery and the support vector machine classifier. *J. Appl. Remote Sens.* **2013**, *7*, 073588. [CrossRef]
33. Kattenborn, T.; Lopatin, J.; Förster, M.; Braun, A.C.; Fassnacht, F.E. UAV data as alternative to field sampling to map woody invasive species based on combined Sentinel-1 and Sentinel-2 data. *Remote Sens. Environ.* **2019**, *227*, 61–73. [CrossRef]
34. Hantson, W.; Kooistra, L.; Slim, P.A. Mapping invasive woody species in coastal dunes in the Netherlands: A remote sensing approach using LIDAR and high-resolution aerial photographs. *Appl. Veg. Sci.* **2012**, *15*, 536–547. [CrossRef]
35. Mori, N. Composition and Structure of Fescue Prairie Respond to Burning and Environmental Conditions More Than to Grazing or Burning Plus Grazing in the Short Term. Master's Thesis, University of Saskatchewan, Saskatoon, SK, Canada, 2009.

36. Archibold, O.W.; Ripley, E.A.; Bretell, D.L. Comparison of the Microclimates of a Small Aspen Grove and Adjacent Prairie in Saskatchewan. *Am. Midl. Nat.* **1996**, *136*, 248–261. [CrossRef]
37. Soubry, I.; Guo, X. Identification of the Optimal Season and Spectral Regions for Shrub Cover Estimation in Grasslands. *Sensors* **2021**, *21*, 3098. [CrossRef]
38. Romo, J.T.; Grilz, P.L.; Redmann, R.E.; Driver, E.A. Standing Crop, Biomass Allocation Patterns and Soil-Plant Water Relations in *Symphoricarpos occidentalis* Hook. Following Autumn or Spring Burning. *Am. Midl. Nat.* **1993**, *130*, 106–115. [CrossRef]
39. Slopek, J.I.; Lamb, E.G. Long-Term Efficacy of Glyphosate for Smooth Brome Control in Native Prairie. *Invasive Plant Sci. Manag.* **2017**, *10*, 350–355. [CrossRef]
40. Baines, G.B.K. Plant Distribution on a Saskatchewan Prairie. *Vegetatio* **1973**, *28*, 99–123. [CrossRef]
41. Statistics Canada 2016 Census-Boundary Files. Available online: https://www12.statcan.gc.ca/census-recensement/2011/geo/bound-limit/bound-limit-2016-eng.cfm (accessed on 20 January 2021).
42. ESA Copernicus Open Access Hub. Available online: https://scihub.copernicus.eu/dhus/#/home (accessed on 8 March 2021).
43. Scott, H.A. *Symphoricarpos occidentalis*. Available online: https://www.fs.fed.us/database/feis/plants/shrub/symocc/all.html (accessed on 16 April 2020).
44. Manske, L.L. *Western Snowberry Biology, 2006 Annual Report, Grassland Section*; Dickinson Research Extension Center: Dickinson, ND, USA, 2006.
45. Schneider, R.E.; Faber-Langendoen, D.; Don Crawford, R.C.; Weakley, A.S. *The Status of Biodiversity in the Great Plains: Great Plains Vegetation Classification*; Supplemental Document 1; U.S. Department of Agriculture, Forest Service, Rocky Mountain Research Station, Fire Sciences Laboratory: Missoula, MT, USA, 1997.
46. Lawrence, D.L.; Romo, J. Tree and shrub communities of woodes draws near the matador research station in Southern Saskatchewan. *Can. Field-Nat.* **1994**, *108*, 397–412.
47. Köchy, M.; Wilson, S.D. Semiarid grassland responses to short-term variation in water availability. *Plant Ecol.* **2004**, *174*, 197–203. [CrossRef]
48. Clarke, S.E.; Tisdale, E.W.; Skoglund, N.A. *The Effects of Climate and Grazing Practices on Short-Grass Prairie Vegetation in Southern Alberta and Southwestern Saskatchewan*; Technical Bulletin; Dominion of Canada, Department of Agriculture: Ottawa, ON, Canada, 1947.
49. Hardy BBT Limited. *Manual of Plant Species Suitability for Reclamation in Alberta*, 2nd ed.; Alberta Land Concervation and Reclamation Council: Edmonton, AB, Canada, 1989. [CrossRef]
50. Hall, J.B.; Hansen, P.L. A Preliminary Riparian Habitat Type Classification System for the Bureau of Land Management Districts in Southern and Eastern Idaho. Available online: https://archive.org/details/preliminaryripar32hall/mode/2up (accessed on 16 April 2020).
51. Hansen, P.L.; Thompson, W.H.; Smith, R.; Yeager, T. Classification and Management of Upland, Riparian, and Wetland Sites of USDI Bureau of Land Management's Miles City Field Office, Eastern Montana USA. *Nat. Resour. Environ. Issues* **2011**, *16*, 32.
52. Bowes, G.G.; Spurr, D.T. Improved forage production following western snowberry (*Symphoricarpos occidentalis* Hook control with metsulfuron methyl. *Can. J. Plant Sci.* **1995**, *75*, 935–940. [CrossRef]
53. Pelton, J. Studies on the Life-History of *Symphoricarpos occidentalis* Hook, in Minnesota. *Ecol. Monogr.* **1953**, *23*, 17–39. [CrossRef]
54. Government of Saskatchewan. *Managing Saskatchewan Rangeland*, 1st ed.; Bruynooghe, J., Macdonald, R., Eds.; Agriculture and Agri-Food Canada: Regina, SK, Canada, 2008.
55. Lackschewitz, K. *Vascular Plants of West-Central Montana-Identification Guidebook*; US Department of Agriculture, Forest Service: Ogden, UT, USA, 1991.
56. Esser, L.L. *Elaeagnus commutata*. Available online: https://www.fs.fed.us/database/feis/plants/shrub/elacom/all.html (accessed on 16 April 2020).
57. Nesom, G. *American Silverberry*—Elaeagnus commutata *Bernh. ex Rydb.*; US Department of Agriculture, Natural Resources Conservation Service: Washington, DC, USA, 1998.
58. Arnold, T.W.; Higgins, K.F. Effects of shrub coverages on birds of North Dakota mixed-grass prairies. *Can. Field-Nat.* **1986**, *100*, 10–14.
59. Pylypec, B. Impacts of fire on bird populations in a fescue prairie. *Can. Field-Nat.* **1991**, *105*, 346–349.
60. Bailey, A.W. Barrier Effect of the Shrub *Elaeagnus commutata* on Grazing Cattle and Forage Production in Central Alberta. *J. Range Manag.* **1970**, *23*, 248–251. [CrossRef]
61. Rowe, J.S. Uses of Undergrowth Plant Species in Forestry Author. *Ecology* **1956**, *37*, 461–473. [CrossRef]
62. Corns, W.G.; Schraa, R.J. Mechanical and Chemical Control of Silverberry (*Elaeagnus commutata* Bernh.) on Native Grassland. *J. Range Manag.* **1965**, *18*, 15–19. [CrossRef]
63. Evans, J.S.; Murphy, M.A.; Ram, K. Package 'spatialEco'—Spatial Analysis and Modelling Utilities; Version 1.3-5; CRAN. Available online: https://github.com/jeffreyevans/spatialEco (accessed on 20 February 2021).
64. Kaufman, Y.J.; Remer, L.A. Detection of Forests Using Mid-IR Reflectance: An Application for Aerosol Studies. *IEEE Trans. Geosci. Remote Sens.* **1994**, *32*, 672–683. [CrossRef]
65. Bhattacharyya, A. On a Measure of Divergence between Two Multinomial Populations. *Indian J. Stat.* **1946**, *7*, 401–406.
66. Bruzzone, L.; Roli, F.; Serpico, S.B. An Extension of the Jeffreys-Matusita Distance to Multiclass Cases for Feature Selection. *IEEE Trans. Geosci. Remote Sens.* **1995**, *33*, 1318–1321. [CrossRef]

67. Jeffreys, H. *Theory of Probability*, 2nd ed.; Clarendon Press: Oxford, UK, 1948.
68. Davis, S.M.; Landgrebe, D.A.; Phillips, T.L.; Swain, P.H.; Hoffer, R.M.; Lindenlaub, J.C.; Silva, L.F. *Remote Sensing: The Quantitative Approach*; Swain, P.H., Davis, S.M., Eds.; McGraw-Hill International Book Co.: New York, NY, USA, 1978; ISBN 007062576X.
69. Gunal, S.; Edizkan, R. Subspace based feature selection for pattern recognition. *Inf. Sci.* **2008**, *178*, 3716–3726. [CrossRef]
70. Shapiro, S.S.; Wilk, M.B. An Analysis of Variance Test for Normality (Complete Samples). *Biometrika* **1965**, *52*, 591–611. [CrossRef]
71. Mohd Razali, N.; Bee Wah, Y. Power comparisons of Shapiro-Wilk, Kolmogorov-Smirnov, Lilliefors and Anderson-Darling tests. *J. Stat. Model. Anal.* **2011**, *2*, 21–33.
72. Huang, H.; Roy, D.P.; Boschetti, L.; Zhang, H.K.; Yan, L.; Kumar, S.S.; Gomez-Dans, J.; Li, J. Separability analysis of Sentinel-2A Multi-Spectral Instrument (MSI) data for burned area discrimination. *Remote Sens.* **2016**, *8*, 873. [CrossRef]
73. Kailath, T. The Divergence and Bhattacharyya Distance Measures in Signal Selection. *IEEE Trans. Commun. Technol.* **1967**, *15*, 52–60. [CrossRef]
74. Campbell, J.E.; Harris, J.R.; Huntley, D.H.; McMartin, I.; Wityk, U.; Dredge, L.A.; Eagles, S. *Remote Predictive Mapping of Surficial Earth Materials: Wager Bay North Area, OPEN FILE 7118 Remote Predictive Mapping of Surficial Earth Materials: Wager Bay North Area, Nunavut—NTS 46-E (N), 46-K (SW), 46-L, 46-M (SW), 56-H (N), 56-I and 56-J (S)*; Geological Survey of Canada: Ottawa, ON, Canada, 2013. [CrossRef]
75. Bindel, M.; Hese, S.; Berger, C.; Schmullius, C. Feature selection from high resolution remote sensing data for biotope mapping. *Int. Arch. Photogramm. Remote Sens. Spat. Inf. Sci.* **2012**, *38*, 39–44. [CrossRef]
76. Lehnert, L.W.; Meyer, H.; Obermeier, W.A.; Silva, B.; Regeling, B.; Thies, B.; Bendix, J. Hyperspectral data analysis in R: The hsdar package. *J. Stat. Softw.* **2019**, *89*. [CrossRef]
77. Tesfamichael, S.G.; Newete, S.W.; Adam, E.; Dubula, B. Field spectroradiometer and simulated multispectral bands for discriminating invasive species from morphologically similar cohabitant plants. *GIScience Remote Sens.* **2018**, *55*, 417–436. [CrossRef]
78. Goslee, S.C.; Havstad, K.M.; Peters, D.P.C.; Rango, A.; Schlesinger, W.H. High-resolution images reveal rate and pattern of shrub encroachment over six decades in New Mexico, USA. *J. Arid Environ.* **2003**, *54*, 755–767. [CrossRef]
79. Cao, X.; Liu, Y.; Cui, X.; Chen, J.; Chen, X. Mechanisms, monitoring and modeling of shrub encroachment into grassland: A review. *Int. J. Digit. Earth* **2019**, *12*, 625–641. [CrossRef]